Proceedings of the Institute of Acoustics

OBLIQUE INCIDENCE DIFFRACTION BY AXISYMMETRIC STRUCTURES

P C Macey

PAFEC Limited, Strelley Hall, Strelley, Nottingham, NG8 6PE

1. INTRODUCTION

Underwater acoustic scattering problems can be analysed using the acoustic boundary element technique, which has been around for some time now. The rapid increase in affordable computer power and the emergence of commercially available software have made this method available to many analysts. However, based on the criteria of three quadratic elements per wavelength, the number of nodes required on a boundary element modelling scattering by a 3D body increases quadratically with the frequency analysed. The time to form the equations and direct solution methods increase as the square and cube of the number of nodes respectively. Thus there is a fairly strict upper limit on the frequency which can be analysed for a given structure using a particular computer.

This paper describes a more efficient technique which is available for scattering by axisymmetric structures. The incident wave is expanded as a Fourier series. Each component is analysed separately using a line element mesh, rather than a surface mesh, and the full 3D pressure field is obtained by combining the circumferential harmonics. Using this technique increases the upper frequency limit for axisymmetric structures.

2. ACOUSTIC EQUATIONS

For small amplitude oscillations in an inviscid, irrotational, compressible fluid, with no mean flow the pressure distribution satisfies the wave equation;

$$\nabla^2 p - \frac{1}{c^2}\frac{\partial^2 p}{\partial t^2} = O \tag{1}$$

where c is the acoustic wavespeed. For steady state oscillations at circular frequency ω, this reduces to the Helmholtz equation ;

$$\nabla^2 p + k^2 p = O \tag{2}$$

where $k = \frac{\omega}{c}$ is the acoustic wavenumber. On a rigid boundary, the condition;

$$\frac{\partial p}{\partial n} = O \tag{3}$$

is satisfied. The pressure p can be decomposed as;

$$p = p_I + p_s \tag{4}$$

where p_I is the free field incident pressure and p_s is the scattered pressure. For external problems, the scattered pressure field must satisfy the Sommerfield radiation condition;

$$\lim_{r\to\infty} r\left|\frac{\partial p_s}{\partial r} - ikp_s\right| = O \tag{5}$$

which ensures that it consists only of outgoing waves.

3. BOUNDARY ELEMENT METHOD

Using the divergence theorem, together with the properties of the free space Green's function;

$$g(\underset{\sim}{x},\underset{\sim}{y}) = \frac{e^{-ikr}}{4\pi r} \tag{6}$$

where $r = |\underset{\sim}{x} - \underset{\sim}{y}|$, the Helmholtz formula can be derived.

$$\varepsilon p(\underset{\sim}{x}) = \int_\Gamma \left(p(\underset{\sim}{y})\frac{\partial g}{\partial n_y}(\underset{\sim}{x},\underset{\sim}{y}) - g(\underset{\sim}{x},\underset{\sim}{y})\frac{\partial p}{\partial n_y}(\underset{\sim}{y}) \right) d\Gamma(\underset{\sim}{y}) + p_I(\underset{\sim}{x}) \tag{7}$$

Where $4\pi\varepsilon$ is the solid angle in the fluid region and n is the normal measured positive into the fluid. To obtain numerical solutions, the surface Γ can be divided into patches over which the pressure and its normal derivative $\frac{\partial p}{\partial n}$ are interpolated using the same shape functions [N]. Equation (7) becomes;

$$\varepsilon p(\underset{\sim}{x}) - \sum_{i=1}^{m}\int_{s_i}\frac{\partial g}{\partial n_y}[N]d\Gamma\{p\} = -\sum_{i=1}^{m}\int_{s_i} g[N]d\Gamma\left\{\frac{\partial p}{\partial n}\right\} + p_I(\underset{\sim}{x}) \tag{8}$$

where s_i is the ith patch of the boundary element and m is the number of patches. $\{p\}$ and $\left\{\frac{\partial p}{\partial n}\right\}$ are vectors of the nodal pressures and pressure normal gradients. Taking the collocation point $\underset{\sim}{x}$ to be at each nodal point in turn a set of linear equations ensue, which can be written in matrix form as;

$$[H]\{p\} = [G]\left\{\frac{\partial p}{\partial n}\right\} + \{p_I\} \tag{9}$$

When the scattering surface is rigid, as in the problems considered in this paper, this simplifies to;

$$[H]\{p\} = \{p_I\} \tag{10}$$

The surface Helmholtz formulation, described above, works well apart from at a characteristic set of frequencies which become dense in the higher frequency range. At these critical frequencies, the surface Helmholtz formulation equations are correct, but they do not possess a unique solution; the matrix $[H]$ is singular and will be ill-conditioned at nearby frequencies. A number of improved boundary element methods are available which overcome these difficulties. The method employed for the analyses in this paper is the CHIEF method, first described by Schenck [1]. The equations of the surface Helmholtz formulation are supplemented by some additional equations, taking $\underset{\sim}{x}$ to be at some interior points in equation (8). The resulting over determined system is then solved in a least squares sense.

4. FOURIER ACOUSTIC BOUNDARY ELEMENTS

If the scattering body is axisymmetric, then the pressure can be expressed as a Fourier series;

$$p(r,\theta,z) = p_o(r,z) + \sum_{m=1}^{\infty}\left(p_m^c(r,z)\cos(m\theta) + p_m^s(r,z)\sin(m\theta)\right) \tag{11}$$

The incident pressure field can be similarly expanded. A Fourier expansion for $\frac{\partial p}{\partial n}$ can be obtained simply by differentiating equation (11) with respect to n throughout. If these Fourier expansions are substituted into equation (7), which is then multiplied by $\cos(m\theta)$ and integrated from $\theta = -\pi$ to $+\pi$, then only one term remains from each series. The resulting equation is:

$$\varepsilon p_m^c(r,z) = \int_S\left(p_m^c(r',z')\frac{\partial g_m(r,z,r',z')}{\partial n'} - \frac{\partial p_m^c}{\partial n'}(r',z')g_m(r,z,r',z')\right)d\zeta(r',z') + p_{\mathrm{Im}}^c(r,z) \tag{12}$$

where ζ is the curve which generates Γ upon revolution about the axis of symmetry and;

$$g_m(r,z,r',z') = \int_{\theta=-\pi}^{+\pi}\cos(m\theta')g(r,o,z,r',\theta',z')d\theta' \tag{13}$$

The contour ζ can be broken down into line elements, which are interpolated over using shape functions, and thus equation (12) can be discretized in a similar form to equation (8) and some matrix equations;

$$[H_m]\{p_m\} = [G_m]\left\{\frac{\partial p_m}{\partial n}\right\} + \{p_{\mathrm{Im}}\} \tag{14}$$

assembled as was done with equation (9). For an equivalent level of discretization, the matrices in equation (14) are much smaller than those of equation (9) and hence much quicker to form and solve. However, this must be done for sufficient terms in the Fourier series to obtain convergence when summed up in equation (11). Even taking these multiple solutions into account, the Fourier method should still provide significant time savings.

The new method has the additional advantage of being more robust when using the CHIEF method in the higher frequency range. It can be proved that the characteristic frequencies at which the surface Helmholtz formulation fails are the eigenfrequencies of the interior region with the Dirichlet boundary condition, see Ref [2]. In the higher frequency range when the eigenfrequencies become dense, a particular frequency being analysed may be close enough to many characteristic frequencies to cause a large loss in the rank of the $[H]$ matrix, see Ref [3]. CHIEF points chosen must avoid the interior nodal surfaces for the eigenmodes of the characteristic frequencies. The number of "good" CHIEF points needed to make the boundary element method work is equal to the loss in rank of the matrices which is not known a priori. Thus in the higher frequency range, it is difficult to know the best number of internal collocation points to use. However, the characteristic frequencies become dense at a much slower rate for the axisymmetric Fourier boundary element resulting in a smaller number of "good" CHIEF points being required.

5. EXAMPLE PROBLEM

The new Fourier acoustic boundary element method was tested by comparison with full 3D analysis results. The test problem was a rigid target consisting of a cylinder with hemispherical endcaps. The cylinder was taken to have length 4m and radius 1m. The surrounding medium was taken as water, with a speed of sound $1500ms^{-1}$. The incident wave was taken to be at an angle 45° to the axis of the cylinder, of unit amplitude and at frequency 1500Hz, see figure 1. The phase of the incident wave was chosen such that the free field pressure at the centre of the cylinder was $e^{i\omega t}$.

6. RESULTS

The problem described above was analysed using three different meshes. A full 3D analysis was performed using the half model illustrated in figure 2. This has 655 nodes and is composed of 96 six-noded triangular quadratic patches and 144 eight-noded quadrilateral quadratic patches. This mesh satisfies the criterion of 3 quadratic elements per wavelength. Five internal CHIEF points were taken. Two axisymmetric meshes were used. Figure 3 shows the coarse axisymmetric mesh, consisting of 20 three-noded quadratic line patches and containing 41 nodes. This has the same axial mesh density as the 3D model. The fine axisymmetric mesh was taken to have twice the mesh density, with 40 quadratic line patches and 81 nodes. Both these models were used with four interior CHIEF points.

Figures 4 and 5 show the variation of the magnitude of the Fourier coefficient at points A and B respectively (see figure 1) computed using the fine axisymmetric mesh. In both cases, there will clearly be very rapid convergence of the Fourier series after the first seven terms. Nine terms would have produced accuracy of a fraction of a percent. Figure 6 shows a comparison between the real part of the pressure along the line AC (see figure 1) in the centre of the shadow zone for the fine axisymmetric and coarse 3D models. Figure 7 gives the same comparison between the two axisymmetric models. Figures 8 and 9 give the same comparisons for the imaginary part of the pressure.

All results are in good agreement. Assuming then that the fine axisymmetric mesh is most accurate, it seems that the coarse axisymmetric model is slightly more accurate than the 3D model. It is also noticeable that the real part of the pressure field seems to be more accurate than the imaginary part.

7. CONCLUSIONS

The Fourier acoustic boundary element method has been shown to work and is capable of producing significant saving on computer time for a full 3D analysis. It does however, require additional post-processing to sum up the Fourier series.

Further work will include using the Fourier acoustic boundary element method to analyse scattering by elastic obstacles.

8. REFERENCES

[1] H. A. Schenck, 'Improved Integral Formulation For Acoustic Radiation Problems'
Jou. Acoust. Soc. Am. Vol.44 No.1 1968 pp 66-75

[2] L. G. Copley, 'Fundamental Results Concerning Integral Representations In Acoustic Radiation'
Jou. Acoust. Soc. Am. Vol.44 No.1 1968 pp 28-32

[3] P. Juhl, 'A Numerical Study Of The Coefficient Matrix Of The Boundary Element Method Near Characteristic Frequencies'
Jou. Sound Vib. Vol.175 No.1 1994 pp 39-50

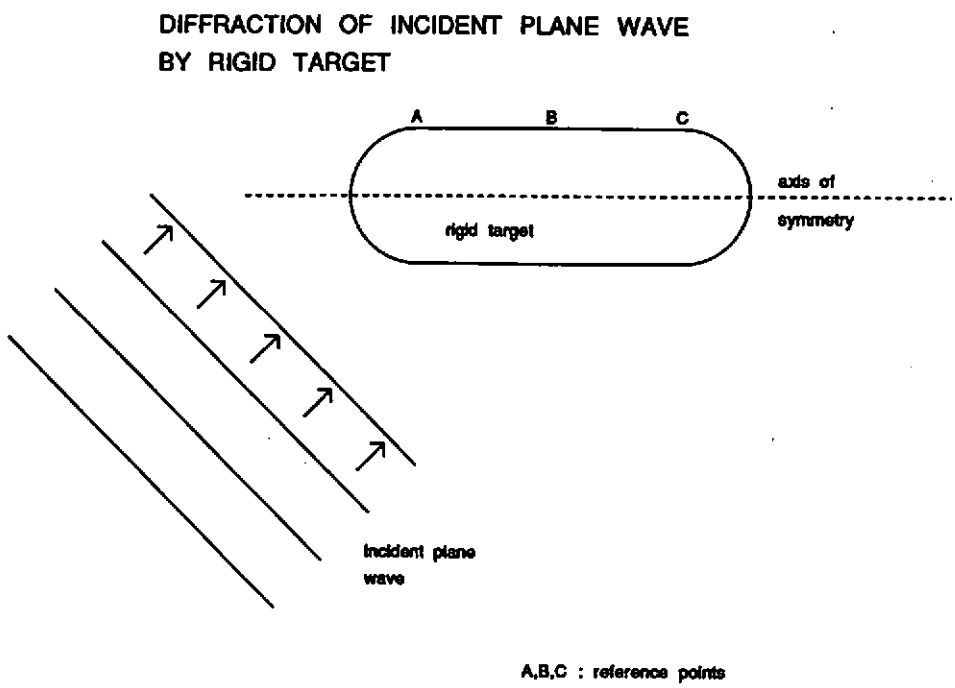

Figure 1

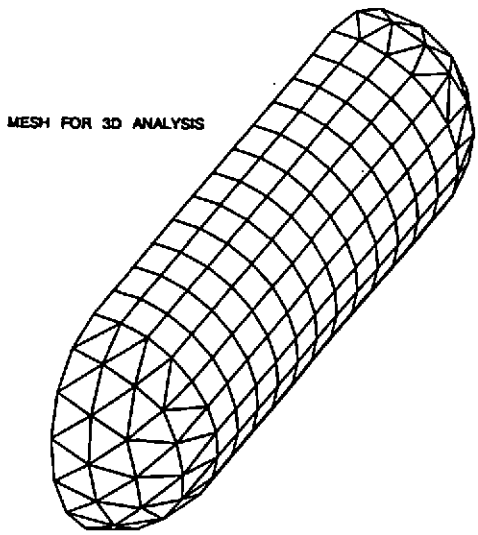

Figure 2

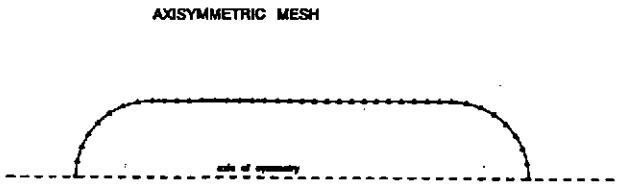

Figure 3

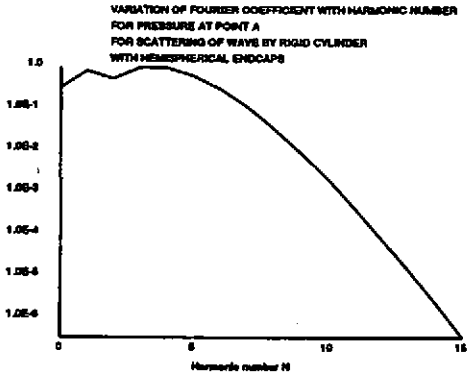

Figure 4

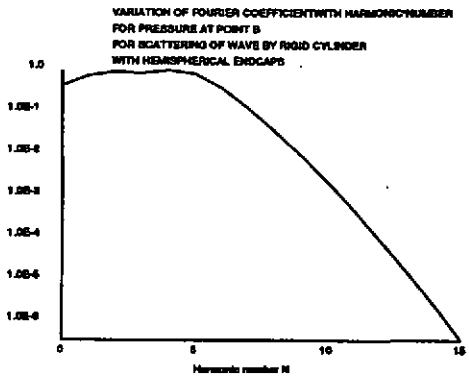

Figure 5

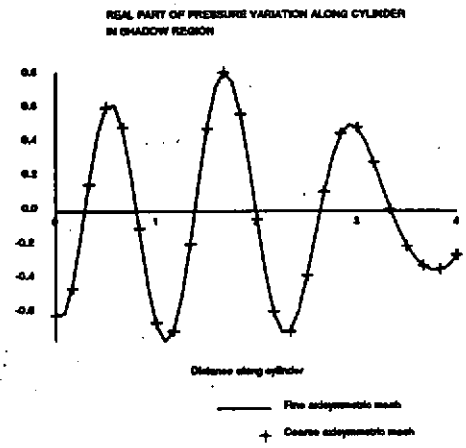

Figure 6

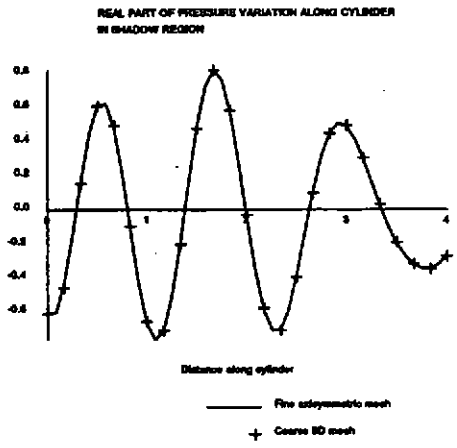

Figure 7

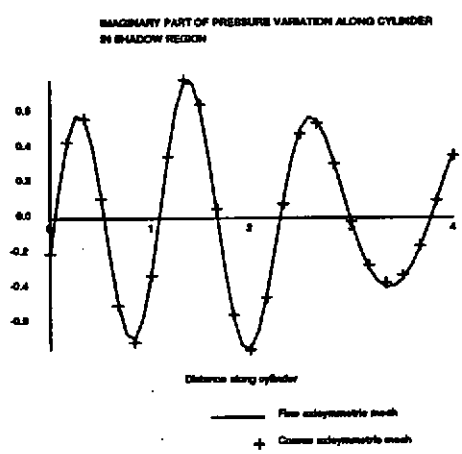

Figure 9

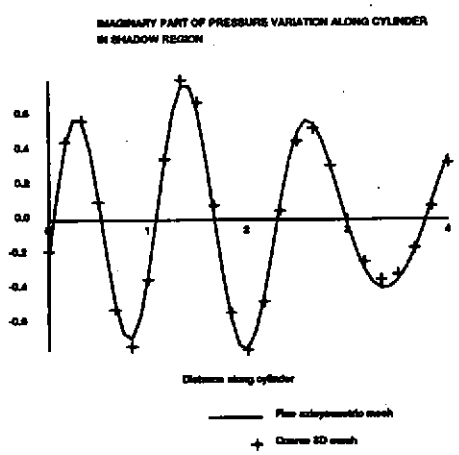

Figure 8